Desalination and Water Treatment
www.deswater.com

doi: 10.1080/19443994.2015.1085452

57 (2016) 17440–17453
August

Taylor & Francis
Taylor & Francis Group

Continuous column study of Cu(II) and Pb(II) ions on alkali-treated coir

Saurabhkumar Singh, Sachin Gondhalekar, Sanjeev R. Shukla*

Department of Fibres and Textile Processing Technology, Institute of Chemical Technology (University under the Section-3 of UGC act 1956), Mumbai 400019, India, Tel. +91 22 3361 1111; Fax: +91 3361 1002; emails: saurabh04567@gmail.com (S. Singh), sachin.gondhalekar@gmail.com (S. Gondhalekar), srshukla19@gmail.com (S.R. Shukla)

Received 6 February 2015; Accepted 15 August 2015

ABSTRACT

Biosorption of Cu(II) and Pb(II) ions by alkali-treated coconut coir (ACC) in a continuous fixed-bed column was carried out from their aqueous solutions. ACC was characterized by FTIR and SEM. The effect of process parameters like bed height, flow rate, and influent initial metal ion concentration was examined. The exhaustion time increased with increase in the bed height and decrease in the flow rate and influent initial concentration. Bohart–Adams, Thomas, and Yoon–Nelson models were found useful for estimating the model parameters of the fixed-bed column, which are valuable for process design as well as to describe the adsorption under changing experimental conditions for predicting the breakthrough curves. Thomas model was the best to fit the breakthrough curves at experimental conditions. The biosorbent was regenerated using 0.01 N NaOH at an eluent flow rate of 10 mL/min and reused up to three times repeatedly without considerable loss in sorption capacity, demonstrating its suitability for commercial application. Sorption of these metal ions from synthetic wastewater has shown excellent potential of ACC for bulk-scale operations.

Keywords: Biosorption; Coir; Fixed-bed column; Modeling; Synthetic wastewater

1. Introduction

The industrial revolution and increased human activities have boosted the discharge of heavy metal ions in the environment, endangering the delicate ecological balance. The heavy metals released in the effluent streams by the battery manufacturing, petroleum refining, electroplating, pigments, and mining industries have harmful effects on water bodies. Due to their non-degradability, toxicity, and high mobility in aqueous medium, the metal ions pass through the food chain and accumulate in the human body, making them prone to a variety of diseases/disorders. Increasing awareness and stringent environmental legislation by the government have forced the industries to maintain the heavy metal discharges below permissible limits [1,2].

Although copper is an important dietary element, its high concentration results in accumulation in liver, and as a consequence abdominal pain, headache, vomiting, nausea, respiratory problems, and ultimately gastrointestinal bleeding occurs [3]. Lead gets easily absorbed in the human body affecting kidneys, gastrointestinal system, physiological, and nervous system [4,5]. The permissible limits of Cu(II) and Pb(II) in wastewater are 2.0 and 0.1 mg/L, respectively [6].

*Corresponding author.

The conventional methods used for metal ion removal suffer from certain drawbacks, such as high operating cost, inadequate reusability, poor efficiency at lower concentrations, and generation of sludge. Biosorption is emerging as an alternative technology for this purpose. It causes passive binding of metal ions on the groups present in naturally abundant biomass. Many agricultural waste products have shown the ability to adsorb large number of heavy metals [2,7,8].

Coir is a cheap lignocellulosic fibrous byproduct acquired from the husks of coconut and produced mainly in tropical countries. It is resistant to harsh wet conditions and chemical and microbial attacks, having highest tear strength among all natural fibers. Cellulose (36–43%), hemi-cellulose (18–20%), and lignin (41–45%) are the major constituents, whereas pectin (2–3%) is a minor constituent; these are known to contain groups responsible for adsorption of metal ions from aqueous solutions [1,9].

We have shown previously that coconut coir, after dyeing with a reactive dye [10] or after oxidative treatment with hydrogen peroxide [11,12] displays enhanced adsorption capacity for the metal ions like Ni(II), Pb(II), Zn(II), and Fe(II). Our recently published work on use of alkali-treated coir [9] as an adsorbent for the removal of Cu(II), Pb(II), Ni(II), and Fe(II) has shown excellent potential for the metal ion adsorption along with complete recovery by desorption, which is further explored here in the form of continuous column study.

Batch experiments are performed to acquire equilibrium sorption isotherms and to determine the maximum sorption capacity of sorbents for metal ions present in aqueous medium. From industrial point of view, however, continuous-flow fixed-bed column is the ideal choice, as it employs the concentration difference to be the driving force for the adsorption of heavy metal ions, thereby resulting in maximum utilization of the biosorption capacity [13].

In this work, we have studied the effect of various operating parameters, including bed height, initial metal ion concentration, and flow rate on the adsorption of Cu(II) and Pb(II) ions on alkali-treated coir fibers at room temperature. Reusability of the column is studied up to three cycles where adsorption, desorption, and regeneration constitute one cycle. An effective, simple, cheap, and environment friendly protocol has been developed to satisfy the industrial needs of metal-free effluent.

Mathematical models for adsorption were used to fit the experimental results obtained from the continuous column experiments. The models are also useful for the scale-up of the biosorption process.

2. Materials and methods

2.1. Biosorbent

Raw coconut coir fibers (RCC), collected from Central Coir Research Institute, Kerala, India, were cut into approximately uniform length of 1 cm, boiled with 1% commercial non-ionic detergent solution, washed with demineralized water, and dried in a hot air oven at 60°C for 24 h.

2.2. Chemicals

$CuSO_4{\cdot}5H_2O$ and $Pb(NO_3)_2$ of analytical reagent grade were supplied by Merck (India) Ltd. Stock solutions of Cu(II) and Pb(II) of approximately accurate 1,000 mg/L concentration were prepared by dissolving appropriate amounts in demineralized water and diluted further to different concentrations. Standard solutions of 1,000 mg/L of Cu(II) and Pb(II) metal ions for Atomic Absorption Spectrometer (AAS) (model-GBC 932 plus, GBC, Australia) were supplied by Merck (I) Ltd. Analytical reagent grade sodium hydroxide and nitric acid, were supplied by SD Fine Chemicals (India) Ltd. Demineralized water was used throughout the experiments.

2.3. Preparation of biosorbent

The coir fibers were treated with 18% (w/v) sodium hydroxide solution at a liquor ratio of 40 at 60°C for 4 h in a stainless steel vessel with continuous stirring. After the treatment, the fibers were washed thoroughly with hot demineralized water till neutral pH and air dried. These were termed as alkali-treated coconut coir (ACC) and used for column experiments.

2.4. Characterization

The FTIR spectra of RCC and ACC were recorded on Shimadzu 8400S FT-IR spectrometer to study the modification in functional groups.

The changes in surface morphology of the biosorbent after alkali treatment were studied using Scanning Electron Microscope (Model-Philips XL-30, The Netherlands). Samples were coated with a thin layer of Au-Pd using a sputter coater to avoid charging, and examined under the SEM at 12 kV with an angle of 45°.

2.5. Fixed-bed column experiments

Continuous flow sorption experiments were conducted in a glass column with an internal diameter of

3 cm and length of 24 cm as shown in Fig. 1. Bottom of the column was first packed with glass wool followed by glass beads (3 mm in diameter) up to a height of 2 cm. ACC fibers were uniformly packed in the column to attain the desired bed heights of 7, 14, and 21 cm, respectively, with care that no air gaps remain. At the top of the column, again glass wool and glass beads were placed to prevent the loss of the biosorbent through flow of solution, and to maintain the packed arrangement of the column intact. Different influent initial concentrations 10, 20, and 30 mg/L of metal ion solutions were used. Upward flow using a peristaltic pump (Electrolab India; Model: PP 201 V) was employed. Cu(II) solution was maintained at pH 4.5 and that of Pb(II) at pH 5.0 by adding 0.1 N NaOH and 0.1 N HNO_3, as these pH values were found to be optimum for adsorption onto coir [9].

The effluent samples were collected from the top of the column at different intervals of time and the residual metal concentration was determined by AAS. The samples were acidified with 0.1 N HNO_3 to avoid precipitation. Breakthrough curves were plotted and operation was stopped on reaching column saturation. All of the experiments were carried out in triplicate at room temperature (30°C), and the mean values were used.

2.6. Regeneration and reusability studies

The ACC column, saturated with metal ion, was washed by passing demineralized water in the upward direction to flush out the unadsorbed metal ions remaining in the bed. The adsorbed metal ions were desorbed by passing 0.15 N HNO_3 at a flow rate of 10 mL/min and the column was washed thoroughly by passing demineralized water till neutral pH. Regeneration was then carried out using 0.01 N NaOH solution followed again by thorough washing. The next cycle of adsorption was conducted by passing 20 mg/L metal ion solution at a flow rate of 10 mL/min in a column of 14 cm bed height and sorption studies were performed. The cycles of sorption–desorption were carried out with an intermediate step of regeneration to estimate the reusability of the biomass.

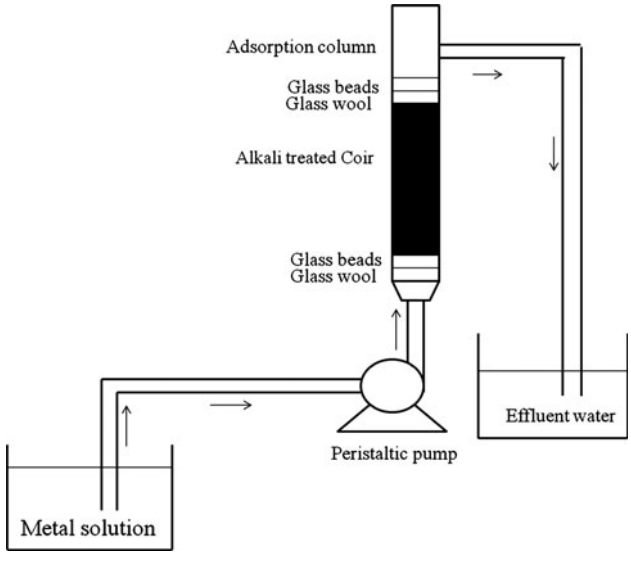

Fig. 1. Schematic diagram of the experimental setup for a column study.

2.7. Modeling and analysis of column data [14–16]

The performance of the packed bed column can be measured by means of breakthrough curve, defined as the ratio of effluent metal concentration to the influent metal concentration as a function of time or volume of the effluent.

Effluent volume can be calculated from the following equation:

$$V_{\text{eff}} = Qt_{\text{total}} \tag{1}$$

The area under the breakthrough curve (A) can be used to find out the total mass of the metal biosorbed for a particular metal concentration and is given by:

$$q_{\text{total}} = \frac{QA}{1,000} = \frac{Q}{1,000}\int_{t=0}^{t=\text{total}} C_{\text{ad}}\,dt \tag{2}$$

where C_{ad} is the concentration of the metal ions adsorbed on coir (mg/L), t_{total} is the total flow time (min), Q is the flow rate (mL/min), and A is the area under the breakthrough curve (cm^2).

Total amount of metal ions sent through the column can be calculated from the following equation:

$$m_{\text{total}} = \frac{C_o Q t_{\text{total}}}{1,000} \tag{3}$$

where C_o is the influent metal ion concentration (mg/L), Q is the volumetric flow rate (mL/min), and t_{total} is the exhaustion time (min).

Total metal removal (%) can be calculated from the ratio of total metal mass sorbed (q_{total}) to the total amount of metal ions sent through the column (m_{total})

$$\text{Total removal } (\%) = \frac{q_{\text{total}}}{m_{\text{total}}} \times 100 \tag{4}$$

Equilibrium metal ion uptake or maximum capacity of the column (mg of metal sorbed/g of sorbent) is given as:

$$q_{eq} = \frac{q_{total}}{w} \quad (5)$$

2.8. Preparation of synthetic wastewater

Synthetic wastewater was prepared containing equimolar concentration of Cu(II) (10.30 mg/L) and Pb(II) (35.42 mg/L) ions by using their respective salts and adding toluene (10 mg/L) as model organic pollutant to generate conditions similar to wastewater generated by industries, wherein organic pollutants are also present along with metal contaminant.

3. Results and discussion

3.1. Characterization

Coir contains around 40% cellulose, as a consequence of which the spectrum largely resembles that of cellulose (Fig. 2). Hydrogen-bonded O–H stretching vibration from the cellulose structure of coir fiber results in a broad and intense peak at 3,400 cm^{-1} in the spectrum. Alkali treatment leads to the disappearance of carbonyl absorption peak of the hemicellulose (1,726 cm^{-1}). An apparent change is observed in the region 1,300–1,200 cm^{-1}, where a broad peak splits into two. Also, a small change in the –OH peak positions in Fig. 2 due to alkali treatment indicates the involvement of –OH groups [17,18].

The existence of pores on the surface of RCC may be noticed from the SEM image (Fig. 3(a)). Upon treatment with the alkali (ACC), these pores open up (Fig. 3(b)) as the soluble components like hemicellulose, tylose, and other fatty acids present therein are removed. This enrichment in porosity with enhanced surface area of coir makes more functional groups available for adsorption, thereby increasing the metal ion uptake. Alkali treatment also results in transforming the smooth surface of raw coir into rough surface with increased accessibility [17].

3.2. Effect of experimental conditions on column adsorption of Cu(II) and Pb(II)

3.2.1. Effect of bed height

Bed height is one of the most important parameters in design of continuous column for metal adsorption. The quantity of biosorbent packed in the column decides the amount of metal ion adsorbed. The packing density of ACC in the column was optimized and fixed at 149 g/L. The breakthrough curves obtained by varying the bed height (7, 14, and 21 cm) at constant initial metal ion concentration (20 mg/L) and flow rate (10 mL/min) for Cu(II) and Pb(II) are shown in Figs. 4(a) and 5(a), respectively. The data on the breakthrough parameters are given in Table 1. The breakthrough time greatly increased for Cu(II) to 613 min from 90 min, and exhaustion time increased to 1,575 min from 645 min on increasing the bed height from 7 to 21 cm. The observation was similar for Pb(II), wherein the breakthrough time increased to 1,999 min from 462 min and exhaustion time increased to 3,204 min from 1,165 min. This has been attributed to increase in the number of binding sites accessible for sorption, resulting in a broadened mass transfer zone (MTZ) [19,20]. The volume of Cu(II) and Pb(II) ion solutions treated also nearly doubled.

The adsorption capacity of the ACC remained nearly constant, 9.0–10.0 mg/g for Cu(II) and 23–24 mg/g for Pb(II) with changing bed height. However, the metal removal efficiency improved with the increase in bed height. According to Singh et al. [21], this might be due to abundant availability of metal ions in the column. Similar results were obtained by Long et al. [22]. The metal removal efficiency of ACC for Cu (II) and Pb(II) increased to 69.46 and 81.20% from 56.98 to 69.83%, respectively, on increasing the bed height from 7 to 21 cm.

The linearization of Bohart–Adams equation and the relationship between the service time (t) and the bed depth of column (Z), called as bed depth-service time (BDST) model was proposed by Hutchins [23]. This is the most extensively used model, according to which the surface reaction between the adsorbate and the residual capacity of the adsorbent governs the rate of adsorption. The BDST model is used to approximate the required bed depth for a given service time. It is given as:

$$t = \frac{N_a}{C_o v} Z - \frac{1}{k_a C_o} \ln\left(\frac{C_o}{C_b} - 1\right) \quad (6)$$

where t is the service time (min), N_a is the adsorption capacity (mg/L), C_o is the initial concentration of solute in the liquid phase (mg/L), v is the influent linear velocity (cm/min); k_a is the rate constant in BDST model (L/mg min), C_b is the effluent concentration of solute in the liquid phase (mg/L), and Z is the bed depth of column (cm).

A plot of t vs. Z yields a straight line, where N_a and k_a can be evaluated. The plots of t vs. Z at 10% breakthrough point for Cu(II) and Pb(II) at a flow rate

Fig. 2. FTIR spectra of raw and alkali-treated coir.

of 10 mL/min are shown in Fig. 6. The plots show linear relationship with R^2 values of 0.999 and 0.992, respectively, representing the viability of BDST model to the adsorption of these ions on a fixed-bed column. The sorption capacities of the bed for Cu(II) and Pb(II) obtained from the slope of BDST plot are 1,020.52 and 3,069.63 mg/L, respectively. The rate constant, k_a, characterizing the rate of solute transfer from the fluid phase to the solid phase, as calculated from the intercept of BDST plot for Cu(II) and Pb(II), is 0.005 and 0.003 L/mg min. In general, even a short bed will avoid breakthrough if k_a is large, but eventually longer bed is required as k_a decreases [24].

The scale up of the process for different flow rates can be done without further experiments by using the BDST model parameters.

3.2.2. Effect of flow rate

The effect of changing flow rates (5, 10, and 15 mL/min) on performance of ACC to adsorb Cu(II) and Pb(II) was studied. The initial concentration was kept at 20 mg/L with bed height 14 cm and room temperature (30°C). The breakthrough curves for Cu (II) and Pb(II) are plotted in Figs. 4(b) and 5(b), respectively, and the results of analysis are given in Table 1. As expected, with increasing flow rate, the breakthrough time and the exhaustion time decreased and the breakthrough curve became steeper for both the metal ions. This might be due to insufficient residence time of the metal ion solution in the column and also due to the diffusion limitations of the solute into the pores of the sorbent [25,26]. The higher flow rate resulted in reduced sorption capacity. Sorption equilibrium could not be achieved at higher flow rate due to short residence time of the metal ions in the column. MTZ increased with the increase in flow rate; similar observation has been reported by Bulgariu et al. [26]. From Table 1, it may be observed that 3.00 and 12.71 L of wastewater can be treated effectively by using 14.80 g of biosorbent in a column of 14 cm bed height at a flow rate of 10 mL/min for Cu(II) and Pb(II), respectively. The higher treatable volume of Pb (II) as compared to Cu(II) proves that ACC has higher sorption capacity for Pb(II) as compared to Cu(II). This may be attributed mainly to ionic radii of metal ions. The Pb(II) ions with larger radii (1.19 Å) have a higher hydration energy and ionic mobility as compared to Cu(II) ions with smaller ionic radii (0.73 Å) [27]. Hydration of metal ions happens owing to the replacement of H_2O ligands of the inner coordination sphere with hydroxo groups. Adsorption occurs as a result of loss of outer hydration sphere. Thus, $Pb(II)_{aq}$ ion, owing to its larger ionic radii, will lose its outer

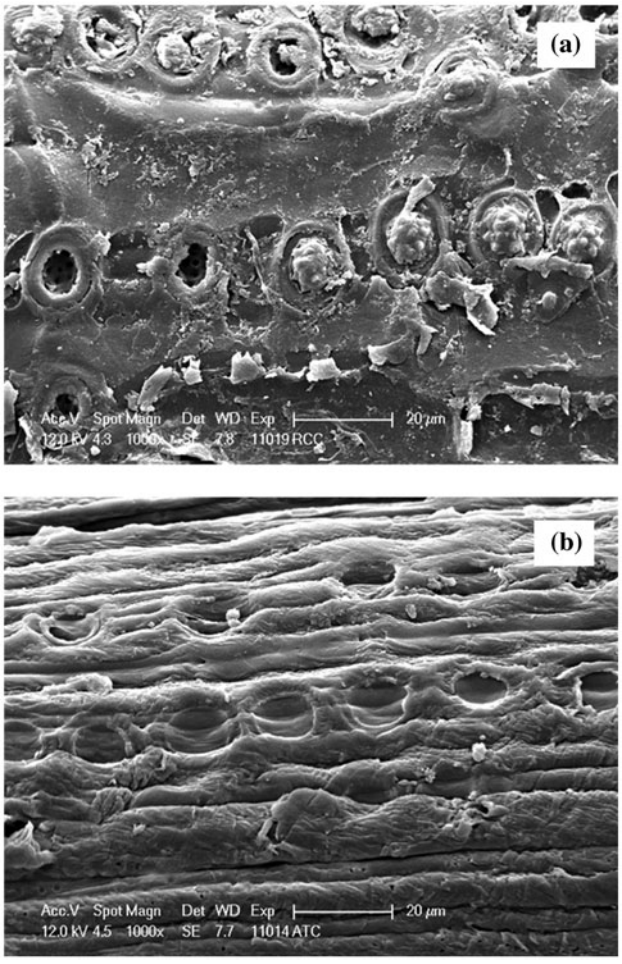

Fig. 3. SEM micrographs of (a) raw and (b) alkali-treated coir.

hydration sphere faster and have a greater access to the binding sites through surface pores compared to Cu(II) ions, leading to higher extent of adsorption [9]. Therefore, minimum flow rate is desirable for the best adsorption performance. Considering the breakthrough time and energy requirements, the optimum flow was taken to be 10 mL/min.

3.2.3. Effect of initial concentration

The breakthrough curves for Cu(II) and Pb(II) ions, on varying the initial metal concentration (10, 20, and 30 mg/L) at a fixed bed height (14 cm) and flow rate (10 mL/min), are shown in Figs. 4(c) and 5(c), and the values for the same are summarized in Table 1. For Cu(II) and Pb(II), the breakthrough occurred at 269 and 809 min for the initial concentration of 30 mg/L, while for the initial concentration of 10 mg/L, it occurred at longer period of 708 and 1,638 min,

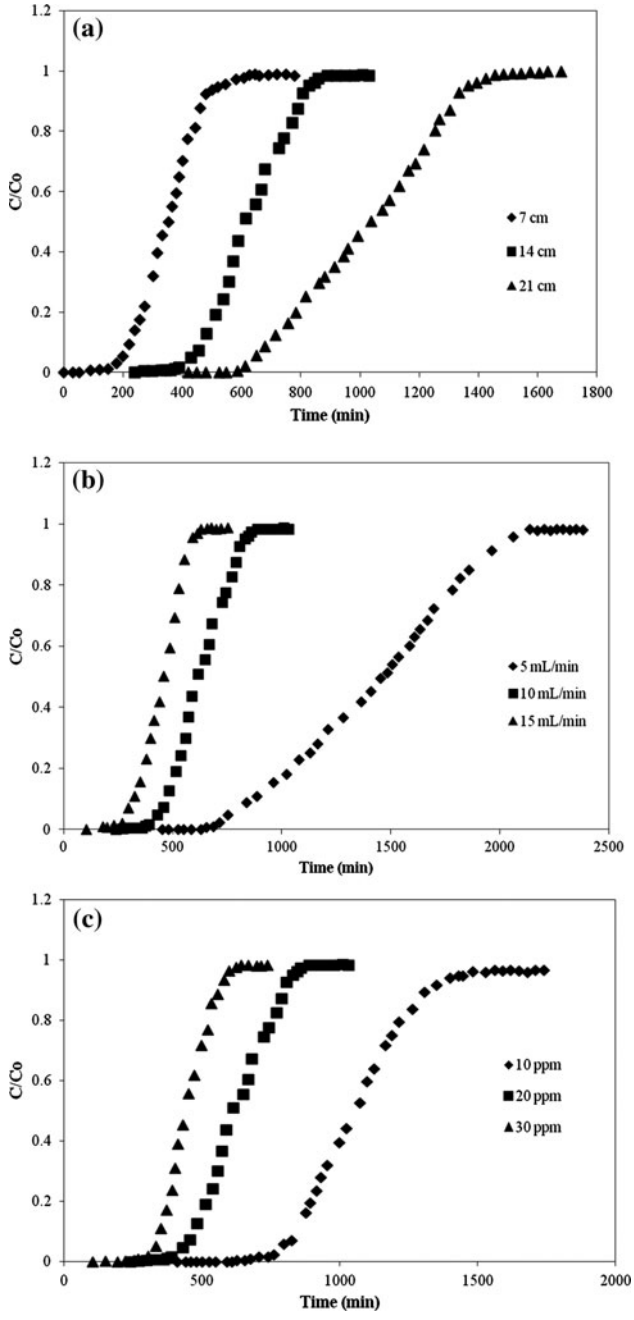

Fig. 4. Breakthrough curves for Cu(II) biosorption onto ACC at different (a) bed heights, (b) flow rates, and (c) initial metal ion concentrations.

proving the inverse relation of breakthrough time and exhaustion time with the initial concentration of metal ions [22]. On the other hand, the sorption capacity increased to 9.23 and 24.54 mg/g from 7.41 and 19.26 mg/g, respectively, for Cu(II) and Pb(II), with increase in the initial concentration from 10 to 30 mg/L. Thus, the faster transport of metal ions, due

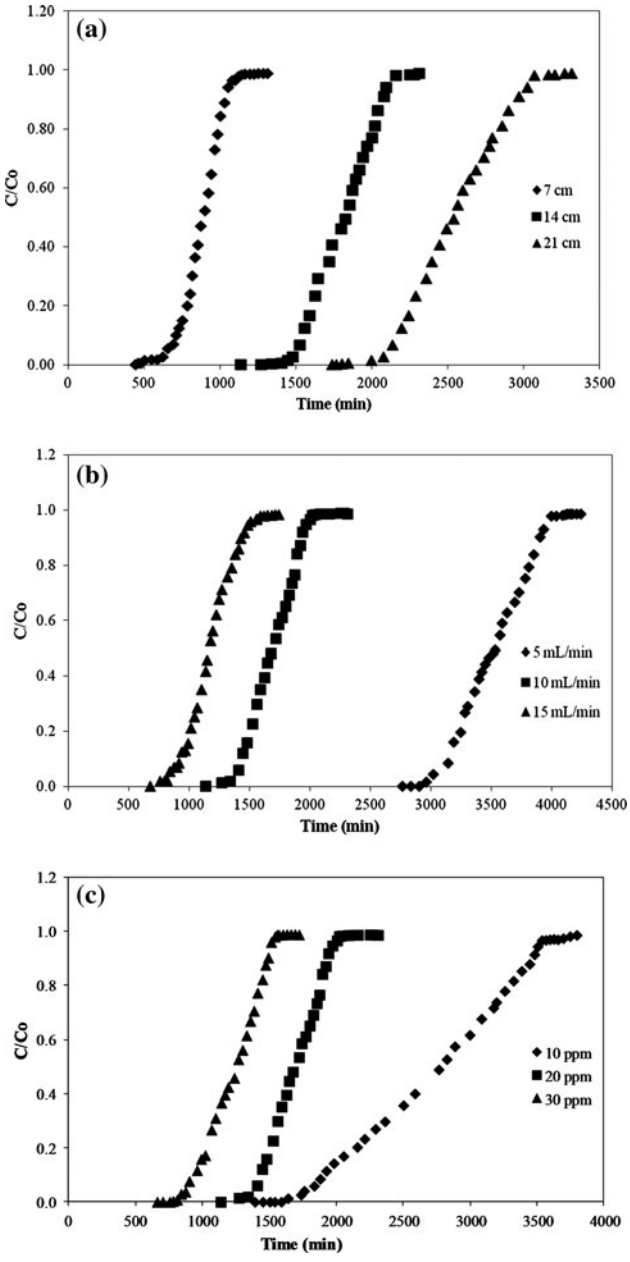

Fig. 5. Breakthrough curves for Pb(II) biosorption onto ACC at different (a) bed heights, (b) flow rates, and (c) initial metal ion concentrations.

to the greater concentration gradient results in a higher mass transfer coefficient, causing the sorbent to saturate rapidly [28]. The volume of Cu(II) and Pb(II) influent treated was maximum viz., 14.84 and 37.45 L at the lowest initial concentration (10 mg/L) due to decreased mass transfer coefficient at low concentration gradient. Steepening and shifting of the breakthrough curve toward origin was observed with the increase in influent concentration for both the metal ions as saturation of binding sites takes place rapidly at higher initial concentration. The steeper the curve, better is the column performance [29]. In case of Cu (II), MTZ increased, whereas in case of Pb(II) it decreased. Longer MTZ at higher initial metal concentration was obtained by Cruz-Olivares et al. [4] whereas shorter MTZ was obtained by Bulgariu et al. [26].

From Table 1, it may be observed that the breakthrough time and sorption capacity of Cu(II) was lower than Pb(II), thus confirming the higher affinity of Pb(II) toward ACC. This observation further leads to the conclusion that adsorption potential of column follows the order Pb(II) > Cu(II).

3.3. Breakthrough curve modeling

Three different models were tried for obtaining the best fit of the column parameters.

3.3.1. Bohart–Adams model

According to this model, the rate of adsorption is proportional to both the concentration of the sorbed substance and the residual capacity of the sorbent. It is used for describing the initial part of the breakthrough curve.

Bohart–Adams model in its linearized form is given by [30]:

$$\ln\left(\frac{C_t}{C_o}\right) = k_{AB}C_o(t) - \frac{k_{AB}N_oZ}{v} \tag{7}$$

where C_t is the effluent concentration (mg/L) at time t (min), k_{AB} is the kinetic constant (L/mg min), C_o is the influent metal concentration (mg/L), N_o is the maximum volumetric sorption capacity (mg/L) of the column, Z is the bed depth of the column (cm), and v is the linear flow rate (cm/min). The values of constants k_{AB} and N_o may be determined with the help of slope and intercept, respectively, from a linear plot of ln (C_t/C_o) vs. t.

These values are given in Table 2. The R^2 values for both the metal ions were found to be above 0.93, which indicates a good fit of experimental data with the model. As expected, with the increase in inlet concentration of Cu(II) and Pb(II) N_o increases, and with the increase in flow rate k_{AB} increases.

Table 1
Biosorption data for fixed-bed ACC column for Cu(II) and Pb(II) adsorption at different process parameters

Process Parameters	t_b (min)	t_e (min)	Z_m (cm)	$V_{eff.}$ (mL)	M_{total} (mg)	M_{ad} (mg)	Removal (%)	q (mg/g)
				Cu(II)				
Bed height Z[a] *(cm)*								
7 (7.49 g)	90	645	6.02	6,450	131.79	75.09	56.98	10.03
14 (14.81 g)	300	950	9.58	9,500	204.04	134.24	65.79	9.06
21 (22.20 g)	613	1,575	12.83	15,750	317.58	220.59	69.46	9.94
Flow rate Q[b] *(mL/min)*								
5	654	2,260	9.95	11,300	246.91	159.18	64.47	10.74
10	300	950	9.58	9,500	204.04	134.24	65.79	9.06
15	180	629	9.99	9,435	188.23	121.05	64.31	8.16
Initial metal ion conc. C_o[c] *(mg/L)*								
10	708	1,484	7.32	14,840	148.55	109.71	73.85	7.41
20	300	950	9.58	9,500	204.04	134.24	65.79	9.06
30	269	643	8.14	6,430	193.09	136.94	70.92	9.23
				Pb(II)				
Bed height Z[a] *(cm)*								
7 (7.49 g)	462	1,165	4.22	11,650	248.15	173.28	69.83	22.94
14 (14.81 g)	1,271	2,082	5.45	20,820	426.81	343.68	80.52	23.22
21 (22.20 g)	1,999	3,204	7.90	32,040	656.82	533.31	81.20	24.02
Flow rate Q[b] *(mL/min)*								
5	2,962	4,131	3.96	41,310	848.01	364.01	42.93	24.60
10	1,271	2,082	5.45	20,820	426.81	343.68	80.52	23.22
15	760	1,506	6.93	22,590	456.32	343.30	75.23	23.27
Initial metal ion conc. C_o[c] *(mg/L)*								
10	1,638	3,745	7.88	37,450	396.67	285.08	71.87	19.26
20	1,271	2,082	5.45	20,820	426.81	343.68	80.52	23.21
30	809	1,555	6.72	15,550	479.13	364.20	76.01	24.54

[a]C_o = 20 mg/L; Q = 10 mL/min.
[b]C_o = 20 mg/L; Z = 14 cm.
[c]Q = 10 mL/min; Z = 14 cm.

Hence, under these circumstances, for improved N_o and smaller k_{AB} (i.e. minimum resistance), the initial metal ion concentrations are required to be higher while the flow rate should be lower.

While this model offers an easy and broad approach to running and estimating sorption-column tests, its authenticity is restricted to the initial range of breakthrough curve.

3.3.2. Thomas model

Thomas model assumes that there is no axial dispersion and that the Langmuir isotherm is the best fit for equilibrium. It is derived with the assumption that the rate driving force obeys second-order reversible reaction kinetics, and is one of the most general and widely used models in column performance theory.

The linearized form of the Thomas model can be expressed as follows [31]:

$$\ln\left(\frac{C_o}{C_t}-1\right)=\frac{k_{Th}q_{Th}M}{Q}-\frac{k_{Th}C_oV}{Q} \tag{8}$$

where C_o is the initial concentration of the metal ion (mg/L), q_{Th} is the adsorption capacity of the system (mg/L), k_{Th} is the Thomas rate constant (L/min mg), M is the mass of the adsorbent in the column (g), Q is the flow rate (mL/min), and V is the volume of metal solution passed through the column (mL). The values

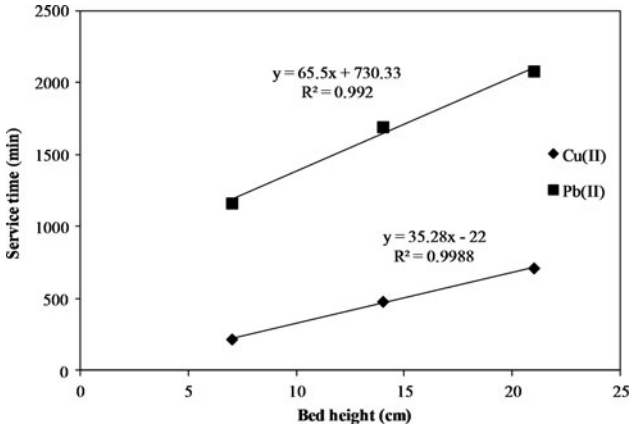

Fig. 6. BDST plot for Cu(II) and Pb(II) sorption onto ACC (C_0 = 20 mg/L; Q = 10 mL/min).

of k_{Th} and q_{Th} can be calculated from the linear plot of ln ($C_o/C_t - 1$) against V.

To determine k_{Th} and q_{Th}, the column data acquired was fitted to the Thomas model and the dynamic sorption of both the metal ions was predicted through the breakthrough curve. Table 2 shows the calculated values of k_{Th} and q_{Th} along with regression coefficients. Furthermore, the calculated uptake values q_{Th} at different operating conditions were almost same as their corresponding experimental ones for both Cu (II) and Pb(II). The high values of R^2 (>0.97) under all working conditions imply that the Thomas model was appropriate for describing the column biosorption data of both Cu(II) and Pb(II) onto ACC. Further, for both the metal ions, with the increase in the bed height, k_{Th} decreased, whereas it increased with increase in the flow rate. The change in q_{Th} with bed height was insignificant. k_{Th} decreased as the influent concentration of Cu(II) ion increased from 10 to 20 mg/L, which agrees with that obtained by Lin et al. [32], but the reverse trend was observed in case of Pb(II) ions. For Pb(II), with increase in the inlet concentration, q_{Th} increased. An excellent agreement between the values of k_{Th} and q_{Th} was obtained from linear and nonlinear parameters. The Thomas model signifies that the diffusion was not the only limiting step and it is an appropriate model for the adsorption process [33,34] Chowdhury et al. [35] found that k_{Th} increases with the increase in flow rate. Yahaya et al. [36] however, observed the reverse.

3.3.3. Yoon and Nelson model

This is the simplest model which does not require detailed data concerning the characteristics of adsorbate, type of adsorbent, and the physical properties of the adsorption bed. This model assumes that the rate of decrease in the probability of adsorption for each adsorbate molecule is proportional to the probability of sorption and the probability of sorbate breakthrough on the sorbent [37].

Linearized form of the Yoon–Nelson model is given as:

$$\ln\left(\frac{C_t}{C_o - C_t}\right) = k_{YN}t - k_{YN}\tau \quad (9)$$

where C_o is the initial concentration of the sorbate (mg/L), k_{YN} is the Yoon−Nelson rate constant (1/min), τ is the time required to reach 50% adsorbate breakthrough (min), and t is the breakthrough sampling time (min). This expression is mathematically equal to Thomas model. The plot of ln ($C_t/C_o - C_t$) vs. t gives a straight line, from which the values of k_{YN} and τ can be determined from the slope and the intercept, respectively.

Different statistical parameters of the Yoon–Nelson model calculated for Cu(II) and Pb(II) are shown in Table 2. With the increase in the flow rate as well as initial concentration, the k_{YN} increased and τ decreased. Higher flow rate results in inefficient adsorption, thus attaining the saturation quickly [38]. On the other hand, with increase in the bed height, the k_{YN} decreased and τ increased. Similar results were obtained by Long et al. [22].

The value of $R^2 > 0.96$ for Cu(II) and >0.95 for Pb (II) indicates best fit of the model for both the metal ion (Table 2).

3.4. Successive cycles of sorption and desorption by column

The regeneration and subsequent reuse of the biosorbent in the sorption process is certainly needed to achieve both process cost reduction and sustainability, and the choice of proper desorption agent is important for this purpose. In our previous work, we have optimized the desorption parameters and the same are used here [9]. The surface characteristics of the biomass are not affected by the acid treatment, but only the bound metal ions are released, maintaining the adsorption capacity almost same. Three successive cycles of adsorption, desorption, and regeneration were repeated to check the feasibility of the removal and recovery process for Cu(II) and Pb(II), as shown in Fig. 7. In both the cases, the desorption of metal ions took place rapidly by using 0.15 N HNO_3 at a flow rate of 10 mL/min. The desorption was almost

Table 2
Bohart–Adams, Thomas, and Yoon–Nelson models parameters for the sorption of Cu(II) and Pb(II) onto ACC

	Parameter			Bohart–Adams			Thomas					Yoon–Nelson				
							Non-linear		Linear			Non-linear		Linear		
	C_o	Z	F	k_{AB} ($\times 10^{-4}$)	N_o	R^2	k_{Th}	q_{Th}	k_{Th}	q_{Th}	R^2	k_{YN}	τ	k_{YN}	τ	R^2
Cu(II)	20	7	10	8.81	1,538.55	0.96	0.82	9.55	0.76	9.87	0.97	0.011	256.37	0.016	350.92	0.99
	20	21	10	2.33	1,564.29	0.95	0.33	9.33	0.42	9.12	0.97	0.013	598.73	0.013	626.27	0.98
	20	14	10	7.87	1,363.87	0.98	0.59	9.08	0.62	9.08	0.98	0.008	955.43	0.008	1,008.18	0.97
	10	14	10	12.09	1,077.23	0.95	0.88	7.15	0.73	7.26	0.96	0.004	753.51	0.010	1,087.78	0.96
	30	14	10	8.83	1,374.22	0.98	0.66	9.03	0.57	9.00	0.96	0.020	443.62	0.017	440.24	0.96
	20	14	5	1.19	1,872.78	0.96	0.18	10.65	0.20	10.41	0.98	0.005	1,448.54	0.005	1,439.54	0.98
	20	14	15	1.65	2,316.62	0.98	0.87	9.13	0.89	9.05	0.97	0.015	372.55	0.019	444.24	0.98
Pb(II)	20	7	10	5.32	4,004.30	0.97	0.63	24.94	0.53	28.15	0.98	0.011	786.51	0.015	880.14	0.99
	20	21	10	3.46	3,509.17	0.94	0.26	23.47	0.32	23.09	0.98	0.011	1,690.69	0.010	1,684.44	0.97
	20	14	10	4.20	3,593.88	0.93	0.39	23.30	0.49	23.21	0.96	0.006	2,402.72	0.007	2,535.23	0.98
	10	14	10	7.84	2,064.96	0.95	0.26	19.60	0.26	18.43	0.95	0.005	2,915.02	0.003	2,570.11	0.95
	30	14	10	1.69	4,204.87	0.95	0.25	25.71	0.32	25.28	0.96	0.013	1,259.51	0.010	1,206.42	0.96
	20	14	5	1.56	3,886.73	0.94	0.25	24.34	0.31	24.29	0.98	0.004	3,219.17	0.006	3,513.75	0.98
	20	14	15	4.11	3,745.04	0.96	0.43	24.00	0.42	24.12	0.99	0.007	1,105.34	0.008	1,173.43	0.99

complete in 30 min with recovery of more than 95% of both the metal ions in consecutive cycles.

The initial concentration of each metal ion (20 mg/L), flow rate (10 mL/min), and bed height (14 cm) for each cycle were kept constant. As the number of cycles was increased, the breakthrough time (t_b) decreased. This is because of the fact that some of the metal ions are irreversibly bound to the surface of the biosorbent.

The regeneration efficiency was determined by using the following equation [39]:

$$\text{Regeneration efficiency } (\%) = \frac{q_{reg}}{q_{org}} \times 100 \quad (10)$$

where q_{reg} is the regenerated column biosorption capacity and q_{org} is the original biosorption capacity, (mg/g of the biosorbent).

The biosorption efficiency progressively decreased, as the sorption/desorption cycles continued (Table 3). The regeneration efficiency decreased nearly to 80% after the third cycle.

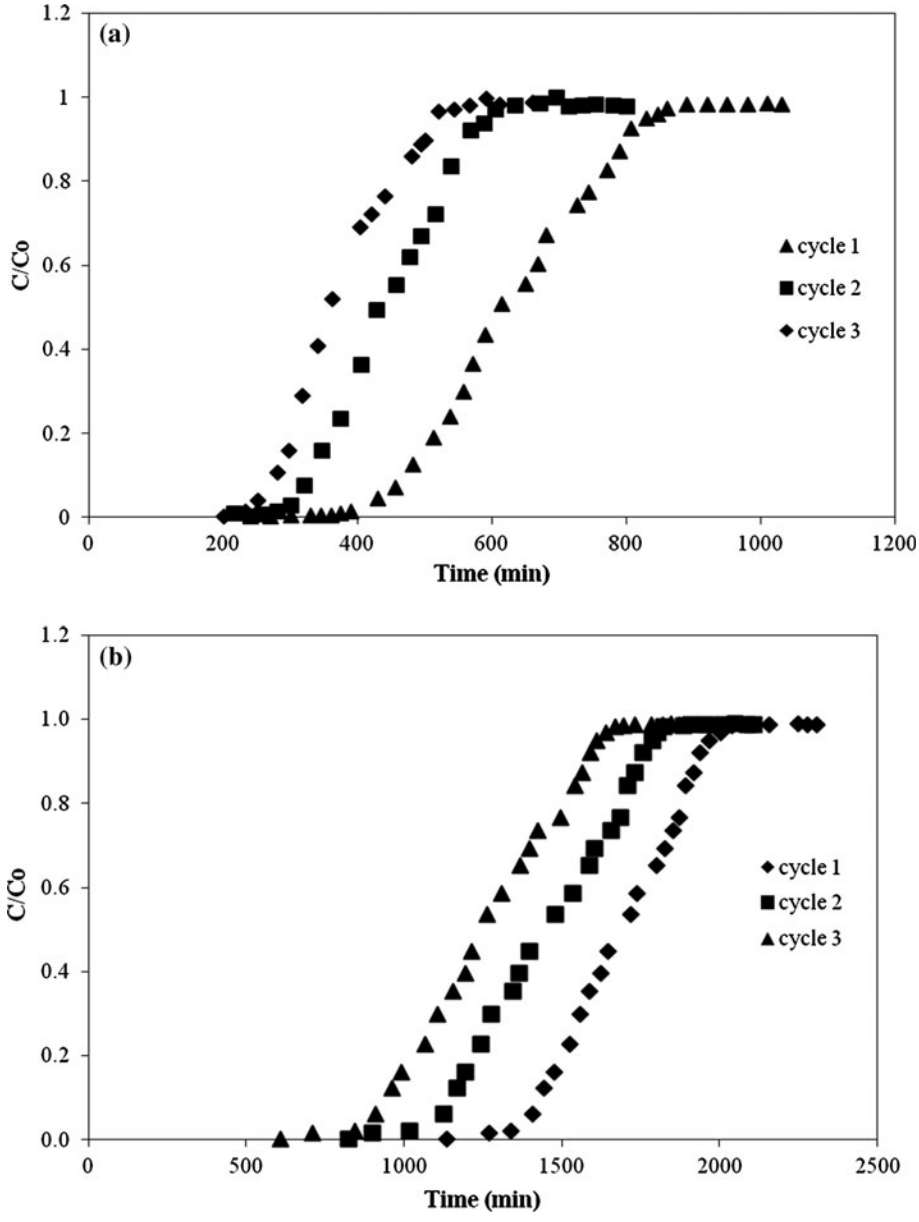

Fig. 7. Breakthrough curves for (a) Cu(II) and (b) Pb(II) adsorption onto ACC during different regeneration cycles: (Co–Cu = 20 mg/L; Co–Pb = 20 mg/L; Q = 10 mL/min; Z = 14 cm).

Table 3
Adsorption process parameters for three adsorption–desorption cycles of Cu(II) and Pb(II) ions (C_o = 20 mg/L; Q = 10 mL/min; Z = 14 cm)

	Cycle no.	Breakthrough time (min)	Exhaustion time (min)	Breakthrough uptake (mg/g)	Regeneration efficiency (%)
Cu(II)	1	300	950	9.06	Original
	2	388	794	8.15	90.00
	3	346	696	7.19	79.36
Pb(II)	1	1,271	2,082	23.22	Original
	2	1,168	1,910	21.32	91.81
	3	964	1,785	19.04	82.00

Table 4
Biosorption data for fixed-bed ACC column in case of synthetic wastewater (Co-Cu = 10.30 mg/L; Co-Pb = 35.42 mg/L; toluene = 10 mg/L; Q = 10 mL/min; Z = 14 cm)

	Biosorption parameters							
Metal ion	t_b (min)	t_e (min)	Z_m (cm)	$V_{eff.}$ (mL)	M_{total} (mg)	M_{ad} (mg)	Removal (%)	q (mg/g)
Cu(II)	324	740	7.87	7,400	76.22	54.796	71.89	3.70
Pb(II)	445	912	7.17	9,120	323.03	240.325	74.40	16.23

3.5. Treatment of synthetic wastewater

Adsorption of metal ions onto ACC column (bed height 14 cm) was conducted using synthetic wastewater at a flow rate 10 mL/min. The composition was: Cu(II) = 10.30 mg/L; Pb(II) = 35.42 mg/L, and toluene = 10 mg/L, and the characteristics were pH 5.55; TDS = 25 mg/L; COD = 25 mg/L, and conductivity = 0.112 mS/cm. The characteristics of wastewater after the adsorption treatment were pH 5.40; TDS = 15 mg/L; COD = 16 mg/L, and conductivity = 0.103 mS/cm.

The breakthrough curves for both Cu(II) and Pb (II), when used as binary mixture are shown in Fig. 8. From Table 1, we can see that when single metal ion solutions of Cu(II) (10 mg/L) and Pb (30 mg/L) were passed through the column of 14 cm at a flow rate of 10 ml/min, adsorption capacity was found to be 7.41 and 24.54 mg/g which reduced to 3.70 and 16.23 mg/g (Table 4) for Cu(II) and Pb(II), respectively, using binary mixture. This can be explained on the basis of competition between Cu(II) and Pb(II) ions for the active sites present on the surface of ACC. The decrease in adsorption capacity in case of Cu(II) is much higher as compared to Pb(II) confirming higher affinity of Pb(II) for ACC. Percentage removal decreased slightly from 73.85 to 71.89% for Cu(II), and from 76.01 to 74.40% for Pb(II), in case of synthetic wastewater as compared to single metal ion solution (Tables 1 and 4). In case of synthetic wastewater, effluent volume treated decreased to 7.40 and 9.12 L from 14.84 to 15.55 L for Cu(II) and Pb(II), respectively (Tables 1 and 4). Breakthrough and exhaustion time were also observed to decrease for biosorption of Cu(II) and Pb(II) in binary metal solution as compared to single metal ion solution. Vimala et al. [40] have also shown that biosorption of metal ion decreases in presence of other ions.

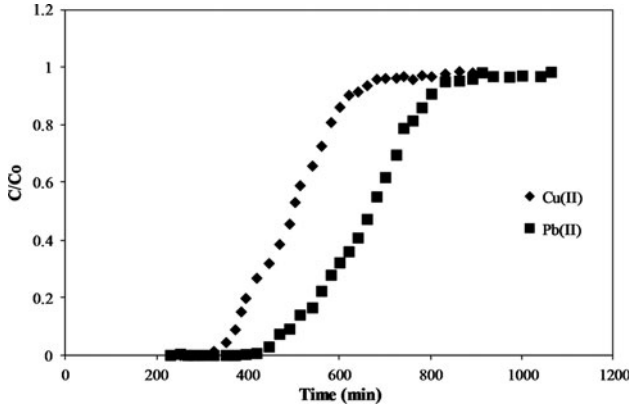

Fig. 8. Breakthrough curves of synthetic wastewater treatment by alkali-treated coir in column (Co–Cu = 10.30 mg/L; Co–Pb = 35.42 mg/L; Q = 10 mL/min; Z = 14 cm).

4. Conclusions

An effective and cheap biosorbent has been produced by simple and eco-friendly alkali treatment of coconut coir fibers for the removal of Cu(II) and Pb(II) ions from their aqueous solutions. The performance of the column packed with ACC in relation to flow rate, influent metal concentration, and bed height was noted. Among the three models chosen, the Thomas model was the best to fit the breakthrough curves at experimental conditions and there was a reasonably good agreement with the experimental data. ACC column has shown excellent reusability, retaining around 80% of its original efficiency, even after three sorption–desorption cycles with intermediate regeneration step using 0.01 N NaOH and with negligible loss of biosorbent. The low price, easy availability, and cheap eco-friendly alkali treatment of coir fiber would make it an attractive biosorbent for heavy metals.

Acknowledgments

The authors Saurabhkumar Singh and Sachin Gondhalekar gratefully acknowledge University Grants Commission, New Delhi for fellowship under Special Assistance Programme.

List of symbols

V_{eff} — effluent volume (mL)
Q — flow rate (mL/min)
t_{total} — total flow time (min)
A — area under the breakthrough curve (cm^2)
C_{ad} — concentration of the metal ions adsorbed on coir (mg/L)
q_{total} — total metal mass sorbed (mg)
m_{total} — total amount of metal ions sent through the column (mg)
w — weight of sorbent (g)
q_{eq} — equilibrium metal ion uptake or maximum capacity of the column (mg of metal sorbed/g of sorbent)
t — service time (min)
N_a — adsorption capacity (mg/L)
k_a — adsorption capacity (mg/L)
C_b — effluent concentration of solute in the liquid phase (mg/L)
Z — bed depth of column (cm)
C_t — effluent concentration (mg/L) at time t (min)
k_{AB} — kinetic constant (L/mg min)
N_o — maximum volumetric sorption capacity (mg/L) of the column
Z — bed depth of the column (cm)
q_{Th} — adsorption capacity of the system (mg/L)
k_{Th} — Thomas rate constant (L/min mg)
M — mass of the adsorbent in the column (g)
V — volume of metal solution passed through the column (mL)
k_{YN} — Yoon–Nelson rate constant (1/min)
τ — time required to reach 50% adsorbate breakthrough (min)
q_{reg} — regenerated column biosorption capacity (mg/g of the biosorbent)
q_{org} — original biosorption capacity (mg/g of the biosorbent)

References

[1] A. Bhatnagar, V.J.P. Vilar, C.M.S. Botelho, R.A.R. Boaventura, Coconut-based biosorbents for water treatment—A review of the recent literature, Adv. Colloid Interface Sci. 160 (2010) 1–15.
[2] V.O. Arief, K. Trilestari, J. Sunarso, N. Indraswati, S. Ismadji, Recent progress on biosorption of heavy metals from liquids using low cost biosorbents: Characterization, biosorption parameters and mechanism studies, Clean—Soil Air Water 36 (2008) 937–962.
[3] G. Blázquez, M.A. Martín-Lara, E. Dionisio-Ruiz, G. Tenorio, M. Calero, Evaluation and comparison of the biosorption process of copper ions onto olive stone and pine bark, J. Ind. Eng. Chem. 17 (2011) 824–833.
[4] J. Cruz-Olivares, C. Pérez-Alonso, C. Barrera-Díaz, F. Ureña-Nuñez, M.C. Chaparro-Mercado, B. Bilyeu, Modeling of lead(II) biosorption by residue of allspice in a fixed-bed column, Chem. Eng. J. 228 (2013) 21–27.
[5] D.N. Lapedes, Encyclopedia of Environmental Science, McGraw Hill Book Company, New York, NY, 1974.
[6] The Environmental Management (Water Quality Standards) Regulations, (2007) First schedule, Permissible limits for municipal and industrial effluents, 20.
[7] K. Kipigroch, M. Janosz-Rajczyk, R. Mosakowska, Sorption of copper(II) and cadmium(II) ions with the use of algae, Desalin. Water Treat. 52 (2014) 3987–3992.
[8] H. Znad, Z. Frangeskides, Chicken drumstick bones as an efficient biosorbent for copper(II) removal from aqueous solution, Desalin. Water Treat. 52 (2014) 1560–1570.
[9] P.M. Shukla, S.R. Shukla, Biosorption of Cu(II), Pb(II), Ni(II), and Fe(II) on alkali treated coir fibers, Sep. Sci. Technol. 48 (2013) 421–428.
[10] S.R. Shukla, R.S. Pai, Comparison of Pb(II) uptake by coir and dye loaded coir fibres in a fixed bed column, J. Hazard. Mater. 125 (2005) 147–153.
[11] S.R. Shukla, R.S. Pai, A.D. Shendarkar, Adsorption of Ni(II), Zn(II) and Fe(II) on modified coir fibres, Sep. Purif. Technol. 47 (2006) 141–147.
[12] S.R. Shukla, V.G. Gaikar, R.S. Pai, U.S. Suryavanshi, Batch and column adsorption of Cu(II) on unmodified and oxidized coir, Sep. Sci. Technol. 44 (2009) 40–62.
[13] N. Miralles, C. Valderrama, I. Casas, M. Martínez, A. Florido, Cadmium and lead removal from aqueous solution by grape stalk wastes: Modeling of a fixed-bed column, J. Chem. Eng. Data 55 (2010) 3548–3554.
[14] M.A. Martín-Lara, G. Blázquez, A. Ronda, I.L. Rodríguez, M. Calero, Multiple biosorption–desorption cycles in a fixed-bed column for Pb(II) removal

by acid-treated olive stone, J. Ind. Eng. Chem. 18 (2012) 1006–1012.
[15] A. Chatterjee, S. Schiewer, Biosorption of cadmium(II) ions by citrus peels in a packed bed column: Effect of process parameters and comparison of different breakthrough curve models, Clean—Soil Air Water 39 (2011) 874–881.
[16] D. Ranjan, M. Talat, S.H. Hasan, Rice polish: An alternative to conventional adsorbents for treating arsenic bearing water by up-flow column method, Ind. Eng. Chem. Res. 48 (2009) 10180–10185.
[17] J. Rout, S.S. Tripathy, S.K. Nayak, M. Misra, A.K. Mohanty, Scanning electron microscopy study of chemically modified coir fibers, J. Appl. Polym. Sci. 79 (2001) 1169–1177.
[18] S. Sreenivasan, P.B. Iyer, K.R.K. Iyer, Influence of delignification and alkali treatment on the fine structure of coir fibres (*Cocos Nucifera*), J. Mater. Sci. 31 (1996) 721–726.
[19] M. Jain, V.K. Garg, K. Kadirvelu, Cadmium(II) sorption and desorption in a fixed bed column using sunflower waste carbon calcium–alginate beads, Bioresour. Technol. 129 (2013) 242–248.
[20] V. Mishra, C. Balomajumder, V.K. Agarwal, Adsorption of Cu(II) on the surface of nonconventional biomass: A study on forced convective mass transfer in packed bed column, J. Waste Manage. 2013 (2013) 1–8.
[21] A. Singh, D. Kumar, J.P. Gaur, Continuous metal removal from solution and industrial effluents using Spirogyra biomass-packed column reactor, Water Res. 46 (2012) 779–788.
[22] Y. Long, D. Lei, J. Ni, Z. Ren, C. Chen, H. Xu, Packed bed column studies on lead(II) removal from industrial wastewater by modified *Agaricus bisporus*, Bioresour. Technol. 152 (2014) 457–463.
[23] R.A. Hutchins, New method simplifies design of activated carbon systems, Chem. Eng. 80 (1973) 133–138.
[24] D.O. Cooney, Adsorption Design for Wastewater Treatment, CRC Press, 1998.
[25] D.C.K. Ko, J.F. Porter, G. McKay, Optimised correlations for the fixed-bed adsorption of metal ions on bone char, Chem. Eng. Sci. 55 (2000) 5819–5829.
[26] D. Bulgariu, L. Bulgariu, Sorption of Pb(II) onto a mixture of algae waste biomass and anion exchanger resin in a packed-bed column, Bioresour. Technol. 129 (2013) 374–380.
[27] R.J. Podolsky, Transport processes in electrolyte solutions[1], J. Am. Chem. Soc. 80 (1958) 4442–4451.
[28] J. Samuel, M. Pulimi, M.L. Paul, A. Maurya, N. Chandrasekaran, A. Mukherjee, Batch and continuous flow studies of adsorptive removal of Cr(VI) by adapted bacterial consortia immobilized in alginate beads, Bioresour. Technol. 128 (2013) 423–430.
[29] G. Naja, B. Volesky, Optimization of a biosorption column performance, Environ. Sci. Technol. 42 (2008) 5622–5629.
[30] G.S. Bohart, E.Q. Adams, Some aspects of the behavior of charcoal with respect to chlorine[1], J. Am. Chem. Soc. 42 (1920) 523–544.
[31] H.C. Thomas, Heterogeneous ion exchange in a flowing system, J. Am. Chem. Soc. 66 (1944) 1664–1666.
[32] L.C. Lin, J.K. Li, R.S. Juang, Removal of Cu(II) and Ni (II) from aqueous solutions using batch and fixed-bed ion exchange processes, Desalination 225 (2008) 249–259.
[33] K. Banerjee, S.T. Ramesh, R. Gandhimathi, P.V. Nidheesh, K.S. Bharathi, A novel agricultural waste adsorbent, watermelon shell for the removal of copper from aqueous solutions, J. Environ. Health Sci. Eng. 3 (2012) 143–156.
[34] S. Chen, Q. Yue, B. Gao, Q. Li, X. Xu, K. Fu, Adsorption of hexavalent chromium from aqueous solution by modified corn stalk: A fixed-bed column study, Bioresour. Technol. 113 (2012) 114–120.
[35] Z.Z. Chowdhury, S.M. Zain, A.K. Rashid, R.F. Rafique, K. Khalid, Breakthrough curve analysis for column dynamics sorption of Mn(II) ions from wastewater by using *Mangostana garcinia* peel-based granular-activated carbon, J. Chem. 2012 (2013) 1–8.
[36] N.K.E.M. Yahaya, I. Abustan, M.F.P.M. Latiff, O.S. Bello, M.A. Ahmad, Adsorptive removal of Cu(II) using activated carbon prepared from rice husk by $ZnCl_2$ activation and subsequent gasification with CO_2, Int. J. Eng. Technol. 11 (2011) 164–168.
[37] Y.H. Yoon, J.H. Nelson, Application of gas adsorption kinetics I, A Theoretical model for respirator cartridge service life, Am. Ind. Hyg. Assoc. J. 45 (1984) 509–516.
[38] M. Calero, F. Hernáinz, G. Blázquez, G. Tenorio, M.A. Martín-Lara, Study of Cr(III) biosorption in a fixed-bed column, J. Hazard. Mater. 171 (2009) 886–893.
[39] V.K. Gupta, S. Sharma, Removal of cadmium and zinc from aqueous solutions using red mud, Environ. Sci. Technol. 36 (2002) 3612–3617.
[40] R. Vimala, D. Charumathi, N. Das, Packed bed column studies on Cd(II) removal from industrial wastewater by macrofungus *Pleurotus platypus*, Desalination 275 (2011) 291–296.